

On rational approximation methods for inverse source problems¹

Martin Hanke² and William Rundell³

Abstract: The basis of most imaging methods is to detect hidden obstacles or inclusions within a body when one can only make measurements on an exterior surface. Such is the ubiquity of these problems, the underlying model can lead to a partial differential equation of any of the major types, but here we focus on the case of steady-state electrostatic or thermal imaging and consider boundary value problems for Laplace’s equation. Our inclusions are interior forces with compact support and our data consists of a single measurement of (say) voltage/current or temperature/heat flux on the external boundary. We propose an algorithm that under certain assumptions allows for the determination of the support set of these forces by solving a simpler “equivalent point source” problem, and which uses a Newton scheme to improve the corresponding initial approximation.

1. Introduction

One of the most basic of inverse problems is to detect hidden objects within a body when one can only make measurements on an exterior surface. The type of problem obtained depends strongly on how the included object interacts with the quantities being measured. The mathematical modeling of electrostatic or thermal imaging methods in non-destructive testing and evaluation leads to inverse boundary value problems for Laplace’s equation and this will be the setting for this paper. Even here there is considerable variation and a vast literature both on questions of uniqueness (how much data is required to make a determination of the object from both geometrical and material considerations) and effective reconstruction algorithms. Even if precise uniqueness results are known, one might be unable to measure the required amount of data. Alternatively, for reasons of expediency one might want a fast algorithm that gives only the salient features of the inclusions such as approximate location and volume rather than a determination of the entire physical

2000 Mathematics Subject Classification. Primary: 35R20.

Key words and phrases. Inverse source problem, rational approximation.

¹ This research was supported by the National Science Foundation under grant DMS-0715060 and by the King Abdullah University of Science and Technology (KAUST) award KUS-CI-016-04.

² Institut für Mathematik, Johannes Gutenberg-Universität Mainz, 55099 Mainz, Germany.
(hanke@math.uni-mainz.de)

³ Department of Mathematics, Texas A&M University, College Station, Tx 77843-3368.

situation. All these problems share a common fact; quite substantial changes in the obstacle can result in extremely small changes in the measured data. In other words, these are severely ill-posed problems. Mathematically this is expressed by the fact that in any of the usual function spaces we would use, the mapping from the unknown object to the measured data is compact and its inversion cannot be bounded. Regularization is therefore a necessity for any workable scheme.

The type of internal object can vary widely - from an inclusion with known boundary condition (for example: Dirichlet, Neumann or impedance type); one where the conductivity varies from the background material (the impedance tomography problem); or an unknown source within the body. This paper will be concerned with the latter situation and our goal will be to examine two problems: the first when we have point sources, the second when the source function has compact support within a finite number of subdomains. From a uniqueness and computational standpoint the case of point sources is relatively well understood and fast reconstruction algorithms are available. The analysis of the second case is much more difficult and if there are multiple included sources, the reconstruction issues are decidedly nontrivial. Our goal in this paper is to show how the solution of the relatively easier first problem can shed light on the more difficult second. The contrasting difficulties between these two problems are to be expected; it is much easier to recover solutions dominated by functions with a localized singularity than the relatively smooth solutions that result from a piecewise continuous right hand side term in Poisson's equation.

Our primary model is therefore the Poisson equation

$$\Delta u = F \quad \text{in } D \tag{1.1}$$

with Cauchy data prescribed on ∂D

$$u = f_d \quad \frac{\partial u}{\partial \nu} = g \quad \text{on } \partial D \tag{1.2}$$

where D is a simply connected domain with smooth boundary ∂D and ν denotes the exterior unit normal of ∂D . We assume that $F \in L^2(D)$ is compactly supported within D : that is $\text{supp } F$ consists of m connected components such that

$$\text{supp } F \subset \Omega = \bigcup_{j=1}^m \Omega_j \tag{1.3}$$

for appropriate simply connected sub-domains Ω_j , $j = 1, \dots, m$, with smooth boundaries, the closures of which are pairwise disjoint. An important subcase is when F is piecewise constant within each Ω_j and this will be the focus of our reconstructions in a later section.

Two remarks should be made. First, the compact support assumption is essential because no matter what type of boundary data is measured, one cannot hope to recover a general function F . One simply has to note that if ϕ is any smooth function with support contained in D , then if F is an admissible source then so also is $F + \Delta \phi$ and since the boundary values of ϕ are identically zero it has no effect on the Cauchy data. Second, if we let w be the harmonic function in D with $w = f_d$ on ∂D then by considering instead the function $u - w$ we can reduce to the case $u = 0$ on ∂D . Thus in contrast to the impedance tomography case, for Poisson's equation one cannot obtain further information by imposing further Cauchy data

(say by changing the input current patterns) as these all condense down to one single data pair due to the linear dependence of the equation on the function F . Thus we are forced to consider the situation of a single Cauchy measurement and we can take the function or values of u on ∂D to be homogeneous. (We refer to Remark 2.1 for a means to avoid an explicit transformation to homogeneous data, in case the given Dirichlet data fail to be homogeneous.)

For problem (1.1), (1.2) and (1.3) there are both uniqueness and non-uniqueness results known. If, for example, $F = \chi(\Omega)$ where Ω is a star-like subset of D then Ω is uniquely determined by the single Cauchy data pair $\{f_d, g\}$, [13, 14]. On the other hand if $F = k\chi(\Omega)$ for k a constant and we integrate (1.1) over D , we obtain $k \int_{\Omega} dx = \int_{\partial D} g ds$ and if Ω is a disk of radius R then it is impossible to obtain *both* the strength k and size of Ω . From the above argument this cannot be resolved by giving further Cauchy data and so all that is possible here is to give some information about the total effective size of Ω . See also [12].

Another special and frequently studied case is when each Ω_j reduces to a single point or when the total integral of the source is order unity and has small source support over a region that we can take to be effectively a disc of diameter ϵ . We now seek to determine both the strengths and locations of a finite number of approximate point sources from the Cauchy data (1.2). These point sources can be modeled as monopoles or dipoles (or indeed poles of arbitrary order):

$$\Delta v = F_M = \sum_{k=1}^M \lambda_k \delta_{z_k} + \mathbf{p}_k \cdot \nabla \delta_{z_k} + \dots \quad \text{in } D \quad (1.4)$$

where $\{z_k\}$ are the locations of the source points, λ_k are the monopole strengths and \mathbf{p}_k are the two dimensional dipole moments. We can view the inverse problem for (1.4) as seeking to determine the location, order and strength of the poles of the function v from Cauchy data information on ∂D . In the two-dimensional case, by considering v as the real part of a meromorphic function from which we have known values on a curve in the complex plane, there is clearly uniqueness for this problem. It is equally clear that we must expect severe ill-conditioning due to the analytic continuation aspect.

The numerical reconstruction of such poles have been considered by others. For example, El Badia and Ha Doung [8] present an algorithm to recover *either* monopole sources *or* dipole sources. The approach is elegant and fast as it effectively decouples the locations and strengths. More recently, Chung and Chung [7] have shown how to combine this approach to reconstruct a mixture of monopole and dipole sources. See also [15].

For the *electrical impedance tomography* problem, there has been a considerable recent work in seeking algorithms that determine location and perhaps the convex support of inclusions. Some of these have involved attempts to turn poles (locations) into inclusions (shape). In particular, the idea of “equivalent dipole sources” plays a role, and one seeks information about an inclusion from a single Cauchy pair as distinct from the usual data set for such problems consisting of the full Dirichlet to Neumann map – or a complete family of Cauchy pairs, [11, 12, 16]. Meromorphic approximation has also played a role in the determination of cracks [5], and small inclusions, [4, 6].

In this paper we will show that the recovery of general multipole sources can be efficiently achieved from general principles. Indeed, for the case of two dimensions

this reduces down to the classic problem of Padé approximation.

As noted, an important subcase of (1.3) is when we know the strength of F within its support and we take this to be of unit value,

$$F_\chi = \chi \left(\bigcup_{j=1}^m \Omega_j \right).$$

In particular, we ask the question: if given the Cauchy data pair (1.2) on ∂D for this problem, and if we use this to reconstruct an approximation v solving (1.4) with nearby Cauchy data, what information do the locations and residues of the poles obtained this way provide about the function F_χ and hence about the sets Ω_j ? Even if we only obtain a rough approximation, and we will see that we can in fact do much better than this, then it may be used as the starting guess for another method such as a Newton scheme. On the other hand such an approximation may suffice – we want to know if something is there and, possibly, with some estimate of location and size.

2. The inverse source problem for the Poisson equation

From this stage on we restrict our discussion to the case that D is the (two-dimensional) unit disk. On the one hand, this is not really a loss of generality, as the general two-dimensional case can always be transformed to the unit disk by means of a conformal transformation. On the other hand the unit disk offers much more powerful computational tools to deal with, as we will see below.

Let u be the solution of the source problem

$$\Delta u = F \quad \text{in } D, \quad u = 0 \quad \text{on } \partial D, \quad (2.1)$$

and denote by

$$g = \frac{\partial u}{\partial \nu} \quad \text{on } \partial D \quad (2.2)$$

the Neumann boundary data of u on ∂D . We assume throughout that $F \in L^2(D)$ has compact support.

In the sequel we identify complex numbers with real vectors from \mathbb{R}^2 , using the corresponding letters from the greek and latin alphabets, respectively, i.e., we identify $\zeta \in \mathbb{C}$ with $z = (\text{Re } \zeta, \text{Im } \zeta) \in \mathbb{R}^2$, and so on. With this convention we define a function f' – for the moment the prime is just part of the notation – of the complex variable $\zeta \in D \setminus \overline{\Omega}$ by

$$f' = \partial_1 u - i \partial_2 u, \quad (2.3)$$

where ∂_1 and ∂_2 denote the partial derivatives with respect to the real and imaginary components of ζ , respectively. The function f' is holomorphic in $D \setminus \overline{\Omega}$; in fact, we cannot resist in quoting Ahlfors [1, p. 163] who wrote:

This, it should be remembered, is the most natural way of passing from harmonic to analytic functions.

From (2.3), (2.1), and (2.2) it follows that

$$\left(\zeta f'(\zeta) \right) \Big|_{\partial D} = \frac{\partial u}{\partial \nu} - i \frac{\partial u}{\partial \tau} = g, \quad (2.4)$$

i.e., that our given Neumann data g are the (real) boundary values of the function $\zeta f'(\zeta)$, and hence, the latter can be extended by reflection to a function that is holomorphic in the neighborhood of ∂D .

Accordingly, $\zeta f'(\zeta)$ admits a Laurent expansion

$$\zeta f'(\zeta) = \frac{1}{2\pi} \sum_{n=-\infty}^{\infty} \alpha_n \zeta^n, \quad r < |\zeta| < 1/r, \quad (2.5)$$

for some $r < 1$, where

$$\alpha_n = \int_0^{2\pi} g(e^{it}) e^{-int} dt = \overline{\alpha_{-n}}, \quad n = 0, 1, 2, \dots \quad (2.6)$$

In particular,

$$\alpha_0 = \int_0^{2\pi} g(e^{it}) dt = \int_D F(x) dx$$

by means of Green's identity.

From (2.5) follows that f' has a (multivalued) antiderivative f given by

$$f(\zeta) = \frac{\alpha_0}{2\pi} \log \zeta + \frac{1}{2\pi} \sum_{\substack{n=-\infty \\ n \neq 0}}^{\infty} \frac{\alpha_n}{n} \zeta^n, \quad r < |\zeta| < 1/r, \quad (2.7)$$

and u coincides with the (well-defined) real part

$$\tilde{u}(x) = \frac{\alpha_0}{2\pi} \log \rho + \frac{1}{2\pi} \sum_{\substack{n=-\infty \\ n \neq 0}}^{\infty} \left(\frac{a_n}{n} \rho^n \cos nt - \frac{b_n}{n} \rho^n \sin nt \right),$$

of f , where $x = (\rho \cos t, \rho \sin t)$, $r < \rho < 1/r$, and $\alpha_n = a_n + ib_n$, $a_n, b_n \in \mathbb{R}$. In fact, this is easy to see, as (2.6) implies that $\tilde{u}(x)$ is vanishing for $\rho = |x| = 1$, and that

$$\frac{\partial \tilde{u}}{\partial \nu}(x) = \frac{\alpha_0}{2\pi} + \frac{1}{2\pi} \sum_{n=1}^{\infty} (2a_n \cos nt - 2b_n \sin nt) = \frac{1}{2\pi} \sum_{n=-\infty}^{\infty} \alpha_n e^{int}$$

for $x = (\cos t, \sin t) \in \partial D$, which coincides with $g(x)$ by virtue of (2.6); accordingly, \tilde{u} and u share the same Cauchy data on ∂D and are harmonic in $D \setminus \overline{\Omega}$, hence are the same on $D \setminus \overline{\Omega}$.

We conclude that the Neumann data of u extend to an analytic complex valued function in $D \setminus \overline{\Omega}$, and even beyond the boundary of D by reflection, namely to $\zeta f'(\zeta)$, and that the real part of the corresponding multivalued function f coincides with u in this very domain.

El-Badia and Ha-Duong [8] approximate the principal part of the Laurent series of f' by a Padé approximation

$$\sum_{n=0}^{\infty} \alpha_{-n} \zeta^{-n-1} \approx \sum_{k=1}^M \frac{\lambda_k}{\zeta - \zeta_k} =: r(\zeta), \quad (2.8)$$

where r is a (complex) rational function with denominator degree M and numerator degree $M - 1$, and the \approx sign is used to signify that the two functions on either side are designed to have the same $2M$ leading terms when developed as power

series in ζ^{-1} . (For a general treatment of Padé approximants we refer to the book of Baker and Graves-Morris [3].) Note that one can conclude from (2.8) by letting $\zeta \rightarrow \infty$ that

$$\alpha_0 = \sum_{k=1}^M \lambda_k. \quad (2.9)$$

It follows from (2.5), (2.6), and (2.8) that

$$\begin{aligned} 2\pi\zeta f'(\zeta) &= \sum_{n=0}^{\infty} \alpha_n \zeta^n - \alpha_0 + \sum_{n=0}^{\infty} \alpha_{-n} \zeta^{-n} \\ &= \frac{1}{\zeta} \sum_{n=0}^{\infty} \alpha_n \zeta^{n+1} - \alpha_0 + \zeta \sum_{n=0}^{\infty} \alpha_{-n} \zeta^{-n-1} \\ &= \frac{1}{\zeta} \sum_{n=0}^{\infty} \overline{\alpha_{-n}} \zeta^{n+1} - \alpha_0 + \zeta \sum_{n=0}^{\infty} \alpha_{-n} \zeta^{-n-1} \\ &\approx \zeta r(\zeta) + \overline{\zeta^* r(\zeta^*)} - \alpha_0, \end{aligned}$$

where $\zeta^* = 1/\bar{\zeta} = \zeta/|\zeta|^2$ is the reflection of ζ at the unit circle. Using (2.9) it is straightforward to see that this yields the (M, M) -Laurent-Padé approximation

$$\zeta f'(\zeta) \approx \frac{1}{2\pi} \sum_{k=1}^M \frac{\lambda_k \zeta}{\zeta - \zeta_k} + \frac{1}{2\pi} \sum_{k=1}^M \frac{\overline{\lambda_k \zeta_k} \zeta}{1 - \bar{\zeta}_k \zeta} \quad (2.10)$$

of $\zeta f'(\zeta)$ introduced by Gragg and Johnson [10]; as a consequence, when $|\zeta| = 1$, the right-hand side of (2.10) is the (M, M) -Fourier-Padé approximation

$$g_M \approx g \quad (2.11)$$

of the Neumann data g , which means that g_M is designed to have the same leading (i.e., low-frequent) $2 \times (2M) + 1$ Fourier modes as g .

From (2.10) we conclude that

$$f'(\zeta) \approx R(\zeta) := \frac{1}{2\pi} \sum_{k=1}^M \frac{\lambda_k}{\zeta - \zeta_k} + \frac{1}{2\pi} \sum_{k=1}^M \frac{\overline{\lambda_k \zeta_k}}{1 - \bar{\zeta}_k \zeta}, \quad (2.12)$$

and hence, its antiderivative is approximated by

$$f(\zeta) \approx \sum_{k=1}^M \frac{\lambda_k}{2\pi} \log(\zeta - \zeta_k) - \sum_{k=1}^M \frac{\overline{\lambda_k}}{2\pi} \log(1 - \bar{\zeta}_k \zeta). \quad (2.13)$$

Assuming that $|\zeta_k| < 1$ for every $k = 1, \dots, M$, it is easy to see that the second sum on the right-hand side of (2.13) is a well-defined holomorphic function of the complex variable $\zeta \in D$, whereas the first sum on the right is multivalued for $\zeta \in D$, in general. Rewriting

$$\lambda_k = \rho_k + i\mu_k, \quad \rho_k, \mu_k \in \mathbb{R}, \quad (2.14)$$

and recalling that u is the real part of f , it follows that

$$u(\zeta) \approx \sum_{k=1}^M \frac{\rho_k}{2\pi} \log |\zeta - \zeta_k| - \sum_{k=1}^M \frac{\mu_k}{2\pi} \arg(\zeta - \zeta_k) + w(\zeta), \quad (2.15)$$

where w is harmonic in D . As

$$\sum_{k=1}^M \mu_k = \operatorname{Im} \sum_{k=1}^M \lambda_k = \operatorname{Im} \alpha_0 = 0$$

by virtue of (2.9), the second term on the right-hand side of (2.15) is harmonic for $|\zeta| > \max |\zeta_k|$.

Remark 2.1: Note that our approach of approximating u via (2.15) only requires the Fourier coefficients of g . Here we show how to get those when the given Dirichlet data (1.2) are inhomogeneous by using the so-called *reciprocity gap functional*, which has been popularized by Andrieux and Ben Abda [2]. Let \hat{u} be any solution of the source problem $\Delta \hat{u} = F$ in D . Then the reciprocity gap functional is defined to be

$$R(w, \hat{u}) = \int_{\partial D} w \frac{\partial \hat{u}}{\partial \nu} ds - \int_{\partial D} \hat{u} \frac{\partial w}{\partial \nu} ds, \quad (2.16)$$

where w is any harmonic function in $H^1(D)$. In particular, choosing $w_n(\zeta) = \zeta^n / (2\pi)$ we obtain

$$R(w_n, \hat{u}) = \frac{1}{2\pi} \int_0^{2\pi} e^{int} \frac{\partial \hat{u}}{\partial \nu}(\cos t, \sin t) dt - n \frac{1}{2\pi} \int_0^{2\pi} e^{int} \hat{u}(\cos t, \sin t) dt = \overline{\alpha_n}.$$

To see this, recall that \hat{u} and u of (2.1) differ by a harmonic function in D , and that R of (2.16) is a linear functional of the second argument, which happens to be zero, when both arguments are harmonic in D . Accordingly,

$$R(w_n, \hat{u}) = R(w_n, u) = \frac{1}{2\pi} \int_0^{2\pi} e^{int} \frac{\partial u}{\partial \nu}(\cos t, \sin t) dt = \alpha_{-n} = \overline{\alpha_n},$$

as was to be shown. This is the version of the method that has been utilized in [8].

Instead of Padé approximations one can alternatively resort to other means of rational approximations. For example, one can think of computing the best approximation of $\zeta f'(\zeta)$ on the unit circle by rational functions with denominator and numerator degrees at most M , either with respect to the maximum norm, or the L^2 -norm. Existence and uniqueness of such rational functions can be established, cf. [5], however, those best approximations are difficult to compute. A numerically feasible alternative are so-called *near best* rational approximations that can be determined from the Adamjan-Arov-Krein theory, cf., e.g., [4].

3. The case of small source supports

Our particular interest is in problems where the source $F \in L^2(D)$ is supported in m individual simply connected components Ω_j as in (1.3), and the individual components are small as compared to D . We will show that in this case the solution u of (2.1) can be approximated by multipole potential series, with their poles being located within the individual components Ω_j of the source support.

To derive this approximation we analyze this situation by selecting points z_j and reference domains O_j such that every O_j contains the origin, and the sets $\Omega_j = z_j + O_j$, $j = 1, \dots, m$, satisfy the requirements of the previous section. Moreover, we choose a reference source $F \in \mathcal{L}^2(D)$ such that

$$\operatorname{supp} F \subset \Omega = \bigcup_{j=1}^m (z_j + O_j). \quad (3.1)$$

Next we introduce a parameter $\varepsilon \in (0, 1)$, and define the family of sources

$$F_\varepsilon(x) = \begin{cases} F(z_j + \frac{x-z_j}{\varepsilon}), & \text{if } x \in z_j + \varepsilon O_j, \\ 0, & \text{else,} \end{cases}$$

and associated solutions u_ε of (2.1) with F replaced by F_ε . Note that, as $\varepsilon \rightarrow 0$, the support of F_ε shrinks to the discrete set $\{z_1, \dots, z_m\}$. It follows that the individual means of F_ε over the m components of

$$\Omega_\varepsilon = \bigcup_{j=1}^m z_j + \varepsilon O_j$$

scale by ε^2 , i.e.,

$$\begin{aligned} \lambda_{j,\varepsilon} &= \int_{z_j + \varepsilon O_j} F_\varepsilon(x) dx = \varepsilon^2 \int_{O_j} F_\varepsilon(z_j + \varepsilon y) dy \\ &= \varepsilon^2 \int_{O_j} F(z_j + y) dy = \varepsilon^2 \lambda_j, \end{aligned} \quad (3.2)$$

where $\lambda_j \in \mathbb{R}$ is the individual mean of the reference source F over $z_j + O_j$. Now we recall the Green's function $G : D \times D \rightarrow \mathbb{R}$ for the Laplace equation in the unit disk, i.e.,

$$G(z, x) = \begin{cases} \frac{1}{2\pi} \left(\log |z - x| - \log \left| \frac{z}{|z|} - |z|x \right| \right) - \frac{1}{2\pi} \log |x|, & x \neq 0, \\ \frac{1}{2\pi} \log |z|, & x = 0. \end{cases} \quad (3.3)$$

Then we can rewrite u_ε as

$$\begin{aligned} u_\varepsilon(z) &= \int_D G(z, x) F_\varepsilon(x) dx \\ &= \sum_{j=1}^m \lambda_{j,\varepsilon} G(z, z_j) + \sum_{j=1}^m \int_{z_j + \varepsilon O_j} (G(z, x) - G(z, z_j)) F_\varepsilon(x) dx \\ &= \varepsilon^2 \sum_{j=1}^m \lambda_j G(z, z_j) + \varepsilon^2 \sum_{j=1}^m \int_{O_j} (G(z, z_j + \varepsilon y) - G(z, z_j)) F(z_j + y) dy \\ &= \varepsilon^2 \sum_{j=1}^m \lambda_j G(z, z_j) + \varepsilon^3 \sum_{j=1}^m \int_{O_j} (\nabla_x G(z, z_j) \cdot y) F(z_j + y) dy + O(\varepsilon^4), \end{aligned}$$

i.e.,

$$u_\varepsilon(z) = \varepsilon^2 \sum_{j=1}^m \lambda_j G(z, z_j) + \varepsilon^3 \sum_{j=1}^m \nabla_x G(z, z_j) \cdot \mathbf{p}_j + O(\varepsilon^4), \quad (3.4)$$

with

$$\mathbf{p}_j = \int_{O_j} y F(z_j + y) dy \in \mathbb{R}^2. \quad (3.5)$$

Here, z is taken from $D \setminus \Omega_\varepsilon$, and the constant in the $O(\cdot)$ -term is independent of z in any compact subset of this set. Also note that the higher order terms in (3.4) contain potentials corresponding to quadrupel and higher order electrostatic poles.

It is easy to deduce in much the same way from (2.12) that the function $f'_\varepsilon(\zeta)$ which is connected to the holomorphic extension of the Neumann boundary values g_ε of u_ε via (2.4) has a similar asymptotic expansion,

$$f'_\varepsilon(\zeta) = \varepsilon^2 \sum_{j=1}^m \frac{\lambda_j}{2\pi} \frac{1}{\zeta - \zeta_j} + \varepsilon^3 \sum_{j=1}^m \frac{\beta_j}{2\pi} \frac{1}{(\zeta - \zeta_j)^2} + O(\varepsilon^4) + h'_\varepsilon(\zeta), \quad (3.6)$$

where $\zeta_j \in \mathbb{C}$ are, again, to be identified with $z_j \in \mathbb{R}^2$, $\beta_j \in \mathbb{C}$ are appropriate coefficients, and for every $0 < \varepsilon < 1$, h'_ε is some holomorphic function in all of D . In fact, from (3.3) follows that h'_ε has a similar expansion in terms of powers of ε , with poles sitting at the reflected positions ζ_j^* in the exterior of the unit disk. In other words, for small source supports the function f is – to a high order of accuracy – a meromorphic function with poles in the points $\zeta_j \in \Omega$ and $\zeta_j^* \in \mathbb{C} \setminus \overline{D}$, $j = 1, \dots, m$.

Remark 3.1: In the particular case when $F = \chi(\Omega)$ then λ_j is the area of O_j , and \mathbf{p}_j/λ_j is the difference between the barycenter of O_j and the origin (or, up to scaling, between the barycenter of Ω_j and the point z_j). More specifically, if the barycenter is itself part of this component, and if we choose z_j as this barycenter, then we obtain $\mathbf{p}_j = 0$, and likewise $\beta_j = 0$, and the third order components in the expansions of u_ε and f_ε vanish.

We can now summarize our findings so far as follows: We have seen in Section 2 that the given Neumann data g of the solution of (2.1) extend to a complex valued function $\zeta f'(\zeta)$, which is analytic in $D \setminus \overline{\Omega}$, and, for the unit disk also extends analytically to an exterior neighborhood of D by reflection. Moreover, when the diameter ε of the source supports is small then the leading order term of the Neumann data is a rational function with denominator degree m , whose poles indicate the locations of the different components of the source support of (2.1).

In this case the Laurent-Padé approximation (2.12) with $M = m$ of f' should not only deliver reasonable approximations of the locations ζ_j , $j = 1, \dots, m$, but also of the numerators in (3.6) when looking at its partial fraction expansion. This information provides the individual means λ_j , $j = 1, \dots, m$. When $F = \chi(\Omega)$ those numbers approximate the volume of the individual inclusions.

If those numerators fail to be positive, however, then this indicates that the asymptotic regime analyzed in this section is not yet valid, and that nearby poles ζ_j whose residues λ_j have cancelling imaginary parts should be gathered to a “cluster of poles” which approximates *one* connected source component. Note that this argument is supported by the fact that the corresponding rational approximation of u is harmonic in every simply connected neighborhood of such a cluster of poles.

4. A numerical algorithm for the case $\Delta u = \chi(\Omega)$

In this section we consider the numerical reconstruction of the domains $\{\Omega_j\}$ from the flux values g on the outer boundary ∂D given by

$$\begin{aligned} \Delta u &= F_\chi = \chi(\Omega) = \chi\left(\bigcup_{j=1}^m \Omega_j\right) && \text{in } D \\ u &= 0, \quad \frac{\partial u}{\partial \nu} = g && \text{on } \partial D. \end{aligned} \quad (4.1)$$

We make the assumption that each Ω_j is starlike with respect to one of its interior points but need only mild assumptions on the boundaries $\partial\Omega_j$; piecewise differentiability will suffice.

There have been many papers devoted to the solution of (4.1) especially in the case of having a single component ($m = 1$). Let \mathcal{F} denote the map from the included region Ω to the values $\frac{\partial u}{\partial \nu} = g$ on ∂D . Newton methods based on a linearization of \mathcal{F} have been a mainstay, but of course require an initial approximation that may be difficult to determine with sufficient accuracy. It was shown in [13] that at each iteration step the Newton scheme preferentially updates the high frequency modes of the basis representation of Ω and so, if adequate information about the suspected low frequency components of Ω is missing due to a poor initial guess, then the scheme will likely fail to converge. However, when it does, convergence is usually quite rapid. A scheme based on Landweber-Fridman iteration does the opposite; at each iteration step it modifies the low frequency modes much more than the high frequency ones. The result is that it does not require as accurate an initial approximation, but the rate of convergence can be exceedingly slow. This is typical of such schemes. However, in an ill-posed problem this slow convergence can be an advantage as it can provide a regularization based on a stopping condition which is often easier to implement than the direct regularization of the derivative map \mathcal{F} , [9]. This is one reason for the popularity of level set methods for inverse inclusion problems. Of course, one can combine these schemes to advantage and with Newton's method there is the option of a step control, albeit at an often considerable increase in the number of iterations. Regardless of the method used, the case of (4.1), especially with $m > 1$, is a nontrivial reconstruction problem and the existing methods require an initial assumption about the locations – either for the scheme to converge or to avoid a large number of iterations (each of which require a direct solve of the partial differential equation).

We therefore approach this problem by first determining the point source problem (1.4) with slightly different Cauchy data, namely

$$\begin{aligned} \Delta v &= F_M := \sum_{k=1}^M \lambda_k \delta_{z_k} && \text{in } D \\ v &= 0, \quad \frac{\partial v}{\partial \nu} = g_M && \text{on } \partial D, \end{aligned} \tag{4.2}$$

where g_M is the (M, M) -Fourier-Padé approximation (2.11) of g , and $z_k, \lambda_k, k = 1, \dots, M$, are the corresponding poles and residues occurring in (2.10) and (2.8). In a second stage, we then use F_M as an initial guess to reconstruct information about the function F_χ and thus the domains $\{\Omega_j\}$ in (4.1). We will see that the resulting distribution of poles and their strengths yield further information that, in fact, goes well beyond simply providing a crude initial approximation.

Returning to (4.2), the first question to be resolved is how to compute the values of $\{z_k\}$, or the associated complex numbers $\{\zeta_k\}$, and $\{\lambda_k\}$. As described in (2.5), (2.6), the Laurent coefficients of the holomorphic function f' are related to the Fourier coefficients of the Neumann data g , and the Laurent-Padé table method allows a determination of the rational function R of (2.12). We can then solve for the ζ_k as the poles of R and λ_k as the corresponding residues. In using this approach one has to be careful in determining an upper bound M to the allowed number of poles, and we will return to this issue below. A convenient way to implement this Padé algorithm, when we are assuming only first order poles for the rational approximation (2.12) to f' , is to use a variation on the El Badia–Ha-Doung approach, [8].

Suppose we have computed $\{\alpha_{-n}\}_{n=0}^{2M-1}$ from (2.6). Then it follows from (2.8) that

$$\alpha_{-n} = \sum_{k=1}^M \lambda_k \zeta_k^n, \quad n = 0, 1, 2 \dots \quad (4.3)$$

Define the diagonal matrix $Z = \text{diag}\{\zeta_1, \dots, \zeta_M\}$ and the vector $\Lambda = [\lambda_1, \dots, \lambda_M]^T$. We now form the $M \times M$ matrices A_ν , $0 \leq \nu \leq M-1$, and the Hankel matrix B to be

$$A_\nu = \begin{bmatrix} \zeta_1^\nu & \zeta_2^\nu & \dots & \zeta_M^\nu \\ \zeta_1^{\nu+1} & \zeta_2^{\nu+1} & \dots & \zeta_M^{\nu+1} \\ \vdots & \vdots & \ddots & \vdots \\ \zeta_1^{M+\nu-1} & \zeta_2^{M+\nu-1} & \dots & \zeta_M^{M+\nu-1} \end{bmatrix}, \quad B = \begin{bmatrix} \alpha_0 & \alpha_{-1} & \dots & \alpha_{1-M} \\ \alpha_{-1} & \alpha_{-2} & \dots & \alpha_{-M} \\ \vdots & \vdots & \ddots & \vdots \\ \alpha_{1-M} & \alpha_{-M} & \dots & \alpha_{2-2M} \end{bmatrix}. \quad (4.4)$$

Thus $A_{\nu+1} = A_\nu Z = A_0 Z^{\nu+1}$, and A_0 is a Vandermonde matrix which, since we assume that the locations of the poles $\{\zeta_k\}$ are distinct, is invertible. We now use the singular value decomposition to ensure that B is invertible – that is, we select M as the greatest integer such that all singular values of B stay above some threshold $\sigma > 0$. This sets the number of poles sought, and can be thought of as a *regularization step* in the procedure.

If we denote the columns of B by the vectors \mathbf{b}_ν (counting from zero to $M-1$), then from (4.3) it follows that $\mathbf{b}_\nu = A_\nu \Lambda$, $\nu = 0, \dots, M-1$. A matrix T is then uniquely defined by

$$TB = \begin{bmatrix} \alpha_{-1} & \alpha_{-2} & \dots & \alpha_{-M} \\ \alpha_{-2} & \alpha_{-3} & \dots & \alpha_{-M-1} \\ \vdots & \vdots & \ddots & \vdots \\ \alpha_{-M} & \alpha_{-M-1} & \dots & \alpha_{1-2M} \end{bmatrix} \quad (4.5)$$

and so $T\mathbf{b}_\nu = \mathbf{b}_{\nu+1}$ for $0 \leq \nu \leq M-1$ where $\mathbf{b}_M = [\alpha_{-M}, \dots, \alpha_{1-2M}]^T$, showing that T is a companion matrix with ones on the super-diagonal and with last row the vector $\gamma = [\gamma_1, \dots, \gamma_M]^T$ where $B^T \gamma = \mathbf{b}_M$. Now

$$\mathbf{b}_{\nu+1} = A_{\nu+1} \Lambda = A_0 Z^{\nu+1} \Lambda = A_0 Z A_0^{-1} A_0 Z^\nu \Lambda = A_0 Z A_0^{-1} A_\nu \Lambda = A_0 Z A_0^{-1} \mathbf{b}_\nu$$

showing that T is also characterized by $T = A_0 Z A_0^{-1}$ and hence has the $\{\zeta_k\}$ as eigenvalues. Computation of these and hence $\{\zeta_k\}$ is straightforward.

Once the points ζ_k have been determined then the residues are easily computed by inverting the Vandermonde matrix A_0 with right hand side \mathbf{b}_0 , $\Lambda = A_0^{-1} \mathbf{b}_0$.

If Ω is a disk of radius ρ then the corresponding “equivalent pole”, in the sense that the same flux value g is obtained, is ζ being equal to the center of Ω and a real-valued residue λ with $\sqrt{\lambda/\pi} = \rho$. This follows directly from the Green’s function for the Laplacian applied to both terms. However, we cannot conclude the converse that real-valued residues must correspond to circular regions. The effect of overlapping regions must be taken into account, and there are certainly counterexamples to the converse. What we can use to advantage is the fact that the strength of a residue does correspond to an area of an equivalent unit source, and so these values can be used as an aid in the next step of the reconstruction process: developing a clustering algorithm that will allow identification of the number and approximate locations of connected components of Ω .

There are many possible clustering algorithms and we will resort to a fairly standard, general purpose one modified for our particular task. We use the correspondence between the pole coefficients (ζ_k, λ_k) and a disk with center ζ_k and radius $\sqrt{|\lambda_k|/\pi}$. We say that the points ζ_{k_1} and ζ_{k_2} (with residues λ_{k_1} and λ_{k_2}) are *connected* if $\sqrt{\pi}|\zeta_{k_1} - \zeta_{k_2}| < |\lambda_{k_1}|^{1/2} + |\lambda_{k_2}|^{1/2}$, that is if the “equivalent disks” overlap. More generally, a set of points $\{\zeta_k\}$, $k \in \mathcal{K}$, is *connected* if for every $k_1 \in \mathcal{K}$ there is a $k_2 \in \mathcal{K}$ such that $\sqrt{\pi}|\zeta_{k_1} - \zeta_{k_2}| < |\lambda_{k_1}|^{1/2} + |\lambda_{k_2}|^{1/2}$. The information in the imaginary part of the residues λ_k assists in this clustering process. Because of the linearity in the form of F we can compute the data g on ∂D for any possible cluster set of poles. Since this has to be a real quantity it follows that the sum of the imaginary parts of the residues of all points ζ_k within a cluster \mathcal{K} must be zero. We can check to see if this holds for our suspected cluster index set \mathcal{K} . In practice we cannot expect this condition to hold exactly, since measurement error in the data and in the numerical approximation of the pole/residue finding algorithm will play a role. On the other hand, M , the total number of detected poles, will not be large unless we have extremely accurate data and so this feature is in fact a viable check.

The final step will consist of synthesizing the information contained in the locations and residues of the poles in the j^{th} subcluster into a geometrical representation of Ω_j . There are several possible ways of doing this but we will only describe one approach that gave good results over a wide range of inclusion geometries. The idea is based on the method of [13] where it was assumed that Ω consists of a single star-like inclusion. First, we compute an approximation for the centroid ω_j of the j^{th} cluster of points coming from running the Pade approximation algorithm. We do not need the value of ω_j precisely and so make the following approximation,

$$\omega_j = \frac{\sum_{k \in \mathcal{K}_j} |\lambda_k| \zeta_k}{\sum_{k \in \mathcal{K}_j} |\lambda_k|}$$

where both sums are over all indices from \mathcal{K}_j that are assumed to correspond to the j^{th} cluster for the component Ω_j .

We note from Remark 3.1 that if this centroid ω_j lies in Ω_j (as we should expect since we are assuming Ω_j is star-like) then by choosing this point as a pole we would lose the associated third order component. This means that we should indeed expect the monopole representation to be a very good approximation.

At this stage we are going to make the assumption, that not only g_M of (4.2) approximates g of (4.1), but also that the solution v_j of

$$\Delta v_j = \sum_{k \in \mathcal{K}_j} \lambda_k \delta_{z_k} \quad \text{in } D, \quad v_j = 0 \quad \text{on } \partial D, \quad (4.6)$$

corresponding to the source points in cluster \mathcal{K}_j , and the solution u_j of

$$\Delta u_j = \chi(\Omega_j) \quad \text{in } D, \quad u_j = 0 \quad \text{on } \partial D, \quad (4.7)$$

have similar Neumann data as well, and this for every $j = 1, \dots, m$. Such an assumption makes sense according to the linearity of the source problem and the asymptotic analysis carried out in Section 3.

Using u_j and v_j of (4.6) and (4.7) we obtain, for any harmonic function h in

D ,

$$\begin{aligned} \int_{\Omega_j} h \, dx &= \int_D (h\Delta u_j - u_j\Delta h) \, dx = \int_{\partial D} h \frac{\partial}{\partial \nu} u_j \, ds \\ &\approx \int_{\partial D} h \frac{\partial}{\partial \nu} v_j \, ds = \int_D (h\Delta v_j - v_j\Delta h) \, dx \\ &= \sum_{k \in \mathcal{K}_j} \lambda_k h(\zeta_k). \end{aligned} \quad (4.8)$$

If we now choose (in complex variables)

$$h(\zeta) = (\zeta - \omega_j)^n, \quad n = 0, 1, 2, \dots,$$

and if we parameterize the boundary of Ω_j as $\omega_j + q_j(\tau)e^{i\tau}$ with q_j a real-valued function of $0 \leq \tau < 2\pi$, then we obtain from (4.8) that

$$\frac{1}{n+2} \int_0^{2\pi} q_j^{n+2}(\tau) e^{in\tau} \, d\tau = \sum_{k \in \mathcal{K}_j} \lambda_k (\zeta_k - \omega_j)^n =: d_{j,n}, \quad n = 0, 1, 2, \dots \quad (4.9)$$

The right hand side $d_{j,n}$ of (4.9) is known in terms of computed point source information, but the equation is, of course, nonlinear in q_j . As in [13] we will solve this by Newton iteration. One iteration step then consists in solving

$$\int_0^{2\pi} q_j^{n+1}(\tau) e^{in\tau} \delta q_j \, d\tau = d_{j,n} - \frac{1}{n+2} \int_0^{2\pi} q_j^{n+2}(\tau) e^{in\tau} \, d\tau, \quad n = 0, 1, 2, \dots, \quad (4.10)$$

for δq_j , and subsequently updating $q_j \rightarrow q_j + \delta q_j$. We can use as a starting guess the constant function $q_j = |\sum_{k \in \mathcal{K}_j} \lambda_k / \pi|^{1/2}$, which corresponds to Ω_j being a disk with center ω_j and corresponding radius. This is exact in the case that the j^{th} cluster contains only a single point, and even in more complex situations this means that we are taking as an initial approximation a region with the approximately correct centroid and area.

We need not take many Newton iterations – there is little to be gained by taking this larger than the number of points in the cluster. We can also use a “frozen” Newton scheme by keeping the value of q_j on the left-hand side of (4.10) fixed at the initial constant; in this version (4.10) gives a formula for the Fourier coefficients of δq . In either scheme effective convergence is achieved within a few iterations.

We also point out that after a few iterations we can, if necessary, update the value of ω_j by computing a better approximation of the barycenter of Ω_j directly from the currently computed boundary curve q_j obtained using (4.10). We never found the need to take this step.

In the above analysis and description we have ignored the possibility of noise in the data except for the regularization step of choosing M poles by selecting a threshold parameter σ . The first observation is that with data noise the point sources obtained from any pole/residue finder may no longer lie within the region D – there is no continuity argument possible that says: if the data error is small enough then the poles $\{\zeta_j\}$ belong to D . As we mentioned before, however, the latter is essential for the algorithm to work. In fact if we try to maximize the information extracted from the data by using low values of σ in order to obtain a larger number of poles, then some of these can lie outside of D . To see this we merely have to take any point within \mathbb{R}^2 , or \mathbb{C} , and assign a source there with

residue λ_ϵ . This single source will contribute a value g_ϵ to the flux on ∂D and by choosing λ_ϵ small enough, we can ensure that $|g_\epsilon|$ is within our assumed data error in g . This situation is easily resolved by assuming a minimum area δA for sources. For a given estimate of the level of noise in g , establish a threshold value for $\lambda_\epsilon = \delta A$ and simply delete all reported poles whose residues are less than λ_ϵ in absolute value. Reducing the dimension M of the system (4.4) according to the two thresholds σ and λ_ϵ , and re-running the code with the reduced number M , the pole-finder algorithm will automatically account for the contribution of the spurious poles. In the reconstructions shown in Figure 2 and Figure 3 we took $\delta A = 10^{-4}$.

We will now illustrate these steps by turning to an actual numerical example. The example chosen shows behaviour typical to many that were tried with a small number of components and similar geometries. It is essential to keep in mind that the more complex a shape that a subregion possesses, the more source points will be needed to represent it and, clearly, the number of required source points will be directly correlated to the number of subregions. Our upper bound of $M = 10$ sets limits here, but in reality the accuracy of the data required to be able to compute even this many points, is far greater than we actually chose (and would be unlikely to be achievable in most practical situations).

Figure 1 shows an inclusion Ω containing three subcomponents; a disk, an ellipsoid, and an apple-shaped region. We have chosen these in part to illustrate certain features of the algorithm. We obtained data by numerically solving the homogeneous Dirichlet problem (2.1) to obtain the corresponding Neumann values $\frac{\partial u}{\partial \nu} = g$. This was accomplished by a quadrature process that was refined until the difference obtained in g was less than 10^{-4} giving a relative error of less than 0.1%. We will view this as “accurate data”. The values of g were output at 64 equally spaced points on the unit circle. Our initial estimate was to allow $M = 10$ possible singular sources. Each of these have four associated real numbers; two each for the coordinates of the locations ζ_k and residues λ_k . This means that we have $4M$ unknowns and need at least this number of data points in order to solve the resulting linear system. Thus our data set, at whatever accuracy, must be considered as relatively “minimal” for implementing the algorithm.

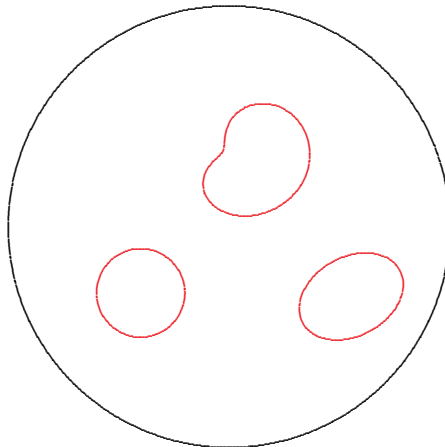


Figure 1. Test obstacles Ω_j

As already mentioned we now implemented the pole finder algorithm with an initial estimate of $M = 10$ poles. Normalizing the singular values of the matrix B so the largest is unity (so that the condition number for B of dimension ν is the reciprocal of the ν^{th} singular value) gives the following singular values for B

$$\begin{array}{cccccc} 1.0 & 0.165 & 0.080 & 3.32 \times 10^{-3} & 5.53 \times 10^{-4} & 3.21 \times 10^{-5} \\ 9.91 \times 10^{-7} & 1.01 \times 10^{-7} & 1.31 \times 10^{-9} & 4.34 \times 10^{-11} & & \end{array} \quad (4.11)$$

Of course, these numbers will depend on the data or, more exactly, on the noise in the data, but the values, although subject to variation, are informative. It is clear

that our hope of recovering ten useful poles was extremely optimistic – at least without obtaining much more accurate data than we are using. On the other hand, on the grounds of (4.11) we should count on obtaining three sources and, unless the data has unexpected types of noise, we should also be able to obtain five. Spectral cut-off equated to maximum level of noise as a choice of regularizing parameter is notoriously conservative, and in fact we might hope to do a little better.

If we take a threshold value of $\sigma = 10^{-2}$ for the singular value decomposition of the matrix B together with the cut-off of 10^{-4} for δA then, as expected from (4.11), this resulted in the number of points being reduced to $M = 3$. The corresponding poles were placed at the approximately correct centroids of the three subinclusions, and the corresponding residuals gave circular approximations with good correlation to the areas of the inclusions.

For approximately $3.3 \times 10^{-3} > \sigma > 5.5 \times 10^{-4}$ we obtained $M = 4$ source points. This is as expected, but now the magnitude $|\lambda|$ for the added point was less than the cut-off value. Thus we still only had three “usable” point sources. In fact, for the data set corresponding to (4.11) this fourth pole came with a residual considerably below the cut-off and, in addition, lay outside of D , showing it was indeed an artifact of the data noise.

A further decrease in σ produced $M = 5$ source points and all of these were now above the cut-off value λ_ϵ . The values of the corresponding ordinates $\{z_k\} \subset \mathbb{R}^2$ and residues $\{\lambda_k\}$ are shown on the left in Table 1. As expected, the disk contains only a single pole which has a real residue. Each of the other two regions have complex-valued residues with the sum of the imaginary parts within each cluster indeed approximately zero.

When σ was decreased to below the 5th singular value, the sixth pole appearing had a residue below the cut-off indicating again a phantom. When σ was chosen less than the next singular value the resulting seven point sources all had magnitudes above the cut-off. The sub-table on the right in Table 1 shows the locations and residues in this case.

On further decrease in σ an eighth point source was placed near the apple-shaped region and had a small, but above cut-off, magnitude. This resulted in a poorer final reconstruction indicating that we had reached, or in fact, exceeded, the limits of this data set.

z_k	λ_k	z_k	λ_k
(-0.400,-0.300)	0.0400 + 0.0000 <i>i</i>	(-0.400,-0.300)	0.0400 - 0.0000 <i>i</i>
(0.631,-0.250)	0.0195 - 0.0063 <i>i</i>	(0.663,-0.241)	0.0089 - 0.0036 <i>i</i>
(0.468,-0.332)	0.0250 + 0.0068 <i>i</i>	(0.437,-0.359)	0.0117 + 0.0050 <i>i</i>
		(0.548,-0.282)	0.0241 - 0.0015 <i>i</i>
(0.137, 0.362)	0.0378 - 0.0138 <i>i</i>	(0.120, 0.365)	0.0324 - 0.0339 <i>i</i>
(0.027, 0.228)	0.0196 + 0.0133 <i>i</i>	(0.078, 0.312)	0.0172 + 0.0265 <i>i</i>
		(-0.010, 0.217)	0.0077 + 0.0075 <i>i</i>

Table 1. Coordinates and residues with $\sigma = 10^{-4}$ and $\sigma = 9 \times 10^{-7}$.

In the leftmost figure of Figure 2 we plot the coordinates and residues (converted to an equivalent disk with radius the square root of $|\lambda_k|/\pi$) when $\sigma = 10^{-4}$. The rightmost figure shows the reconstruction using the scheme (4.10) and formula (4.9).

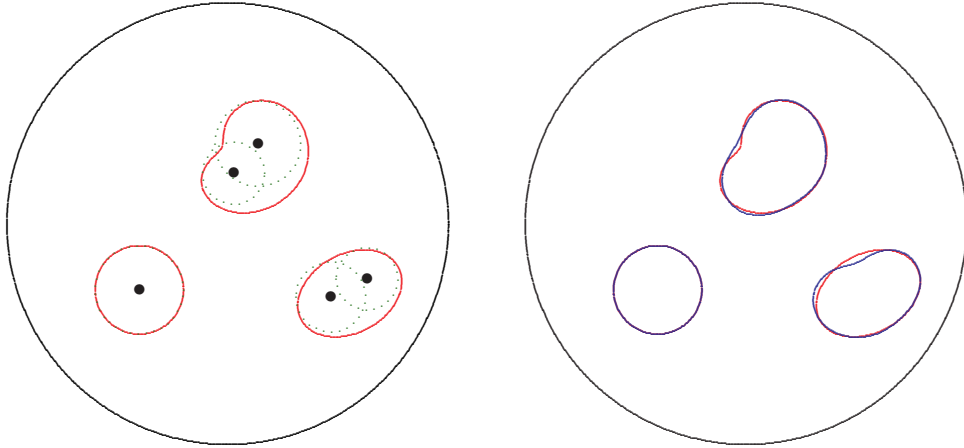


Figure 2. Equivalent pole coordinates/residues, reconstruction, $\sigma = 10^{-4}$.

Figure 3 shows the corresponding reconstruction using $\sigma = 9 \times 10^{-7}$. As noted, this represents the best reconstruction that we could obtain with this particular data set.

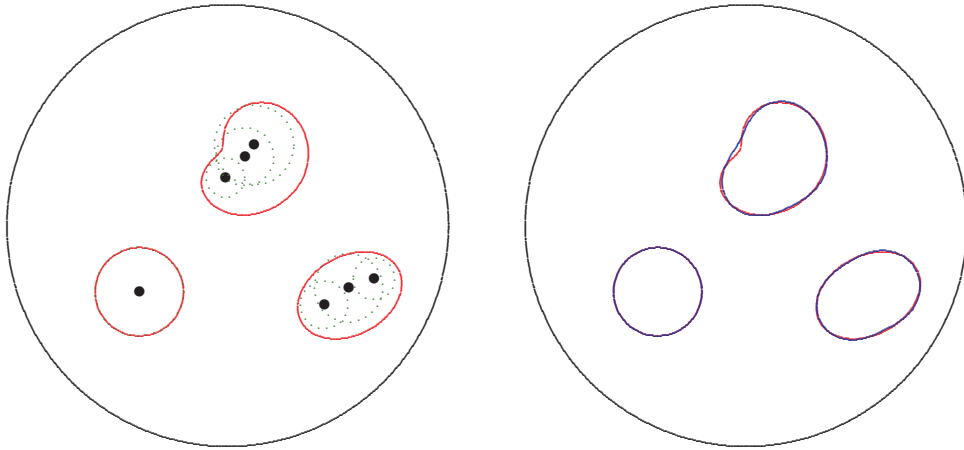


Figure 3. Equivalent pole coordinates/residues, reconstruction, $\sigma = 9 \times 10^{-7}$.

One of the questions to be resolved in any reconstruction process is the choice of the regularization parameter – and the rationalization behind this choice. In obtaining the above reconstructions we have actually used three parameters. The first of these is σ and while the “correct value” here must depend on the amount and type of the error in the data, it is not clear how to directly correlate these. The number M of poles obtained is certainly a nonlinear function of σ , but as (4.11) shows, the coupling between M and σ allows for considerable latitude in σ and this should be viewed as an advantage. The second parameter δA is used to determine whether a located pole has significant residue or is considered a phantom directly due to noise in the data. The choice of δA is much more transparent and is based on the largest circular source that would contribute an amount to the flux data less than the estimated error in this quantity. Failure to delete such small quantities would have only a small effect on the reconstructions of the larger regions and the

practice described above is to re-run the pole/residue finder with the decreased value of M to include these small contributions (or possibly artifacts of the data). For these reasons the choice of δA is not critical: indeed, with our particular data set, a choice of δA one order of magnitude in either direction of the selected value would not have changed the number of poles used for σ values corresponding to $M \leq 7$. Finally, there is the regularization in the Newton scheme used in (4.10) and formula (4.9). This is less of an issue since we have relatively few poles per inclusion and can only recover a few modes of each q_j ; the number of Newton iterations is never going to be large. We never found regularizing this step to be necessary. An exception might be if there is a single source inclusion with a complex shape and accurate enough data, so that we might be able to use the contributions from a relatively large number of poles.

What if we had greater noise in the data or were forced to measure at fewer points on ∂D ? In the latter case, as explained earlier, this would limit the number of admissible poles M . This may still provide sufficient information for a good reconstruction when Ω consists of only one single component, or when the two or three components of Ω have nearly circular geometry, but otherwise this would be a major limitation. If the data noise were to increase we would be forced to increase σ and this in turn would limit the number of poles obtained as we require the matrix B of (4.4) to be numerically invertible. We would also be forced to increase the cut-off value of λ which would decrease the number of useful poles as well as introduce further errors in both their strengths and locations. For example, with 1% Gaussian noise with mean zero, we would be on the borderline to being able to obtain only five usable poles and, therefore, at best would be able to obtain a reconstruction somewhat poorer than that of Figure 2.

Finally, we have assumed throughout that $D \subset \mathbb{R}^2$ but this is not an essential restriction. As was proposed in [8], we can determine sources in three dimensions by applying the two-dimensional algorithms in each of three projected planes. The clustering algorithm works much as before and the Newton scheme in (4.10) adapts directly to higher spatial dimensions.

5. References.

- [1] L. V. Ahlfors. *Complex Analysis*. McGraw-Hill, New York, third edition, 1979.
- [2] S. Andrieux and A. Ben Abda. Identification of planar cracks by complete overdetermined data: inversion formulae. *Inverse Problems*, 12:553–563, 1996.
- [3] G.A. Baker and P. Graves-Morris. *Padé Approximants*. Cambridge University Press, Cambridge, second edition, 1996.
- [4] L. Baratchart, A. Ben Abda, F. Ben Hassen, and J. Leblond. Recovery of pointwise sources or small inclusions in 2D domains and rational approximation. *Inverse Problems*, 21:51–74, 2005.
- [5] L. Baratchart, J. Leblond, F. Mandréa, and E.B. Saff. How can the meromorphic approximation help to solve some 2D inverse problems for the Laplacian? *Inverse Problems*, 15:79–90, 1999.
- [6] D.J. Cedio-Fengya, S. Moskow, and M.S. Vogelius. Identification of conductivity imperfections of small diameter by boundary measurements. Continuous

- dependence and computational reconstruction. *Inverse Problems*, 14:553–595, 1998.
- [7] Y.-S. Chung and S.-Y. Chung. Identification of the combination of monopolar and dipolar sources for elliptic equations. *Inverse Problems*, 25:085006, 2009.
- [8] A. El Badia and T. Ha-Duong. An inverse source problem in potential analysis. *Inverse Problems*, 16:651–663, 2000.
- [9] H. Engl, M. Hanke, and A. Neubauer. *Regularization of Inverse Problems*. Kluwer Academic Publishers, Dordrecht, 1996.
- [10] W.B. Gragg and G.D. Johnson. The Laurent-Padé table. In *Information Processing 74, Proceedings IFIP Congress*, pages 632–637. North-Holland, Amsterdam, 1974.
- [11] M. Hanke. On real-time algorithms for the location search of discontinuous conductivities with one measurement. *Inverse Problems*, 24:045005, 2008.
- [12] M. Hanke, N. Hyvönen, M. Lehn, and S. Reusswig. Source supports in electrostatics. *BIT*, 48:245–264, 2008.
- [13] F. Hettlich and W. Rundell. Iterative methods for the reconstruction of an inverse potential problem. *Inverse Problems*, 12:251–266, 1996.
- [14] V. Isakov. *Inverse Problems for Partial Differential Equations*. Springer-Verlag, New York, second edition, 2005.
- [15] H. Kang and H. Lee. Identification of simple poles via boundary measurements and an application of EIT. *Inverse Problems*, 20:1853–1863, 2004.
- [16] O. Kwon, J.K. Seo, and J.R. Yoon. A real time algorithm for the location search of discontinuous conductivities with one measurement. *Comm. Pure Appl. Math.*, 55:1–29, 2002.